https://doi.org/10.2478/acph-2025-0023

Short communication

α-Heteroarylthiomethyl ketones: Small molecule inhibitors of 3CL^{pro}

DAMIJAN KNEZ[1,*]

MATIC PROJ[1]

KRIŠTOF BOZOVIČAR[2]

STANISLAV GOBEC[1,*]

[1] *University of Ljubljana, Department of Pharmaceutical Chemistry, Faculty of Pharmacy, 1000 Ljubljana, Slovenia*

[2] *University of Ljubljana, Department of Pharmaceutical Biology, Faculty of Pharmacy, 1000 Ljubljana, Slovenia*

ORCID: Damijan Knez, https://orcid.org/0000-0001-9917-1384; Matic Proj, https://orcid.org/0000-0003-4043-9686; Krištof Bozovičar, https://orcid.org/0000-0003-0025-1734; Stanislav Gobec, https://orcid.org/0000-0002-9678-3083.

[*] Correspondence; e-mails: damijan.knez@ffa.uni-lj.si; stanislav.gobec@ffa.uni-lj.si

ABSTRACT

The main protease 3CL^{pro} of the SARS-CoV2 virus is a well-established therapeutic target for the treatment of Covid-19. In this study, we screened an *in-house* compound library and identified a series of α-heteroarylthiomethyl ketones as inhibitors of 3CL^{pro}. Among these, analogues **31** and **33** emerged as the most interesting candidate with IC_{50} values of 95.4 ± 3.1 and 95.0 ± 6.9 μmol L^{-1}, respectively. Preliminary *in vitro* studies suggest a potential covalent mode of inhibition, although further studies are required to confirm this mechanism. These findings provide a new chemical scaffold for the development of 3CL^{pro}-targeting inhibitors.

Keywords: SARS-CoV-2, 3CL^{pro} inhibitors, main protease, covalent inhibitors, ketones

Accepted June 6, 2025
Published online June 9, 2025

INTRODUCTION

Coronaviruses (CoVs) are pleomorphic enveloped positive-strand RNA viruses with unusually large genomes, comprising approximately 30 kilobases. Although they are endemic in the human population and account for 10–30 % of common colds, they were not considered a threat to human health since they mainly cause respiratory infections with mild symptoms (1). However, this view changed with the realization that CoVs are maintained in an animal reservoir and that their transmission to humans is possible *via* intermediate hosts (2). At the end of 2019, Wuhan, China, became a hotspot for the uncontrollable spread of the SARS-CoV-2 virus (3). SARS-CoV-2 reached all parts of the world and caused COVID-19, the most severe pandemic of modern times (4). Both viral and host peptidases play important roles in key steps of coronaviral infection and replication processes (5). Peptidases encoded in the viral genome are essential for processing replicase polyproteins and evading the host immune response, while host peptidases are involved in various steps of viral uptake into the host cell. The viral genome encodes one or two cysteine peptidases, the papain-like peptidase (PLP) and chymotrypsin-like cysteine 3C-like peptidase – 3CL^{pro}, both of which are pivotal for transcription of the viral genome and its replication (6). 3CL^{pro} consists of three domains: domains 1 and 2 form the chymotrypsin-like fold, while domain 3 is required for dimer formation and affects catalytic activity through dynamically controlled allostery (7). Among viral

peptidases, 3CL^{pro} is an attractive target for the development of antiviral drugs against SARS-CoV-2 and other CoVs, because of its essential role in post-translational polyprotein processing. Numerous inhibitors of 3CL^{pro} peptidase have been developed (8–11), and nirmatrelvir was the first-in-class inhibitor approved by regulatory agencies in combination with ritonavir under the trade name Paxlovid^{TM} for the treatment of mild-to-moderate COVID-19 in adults (12). Nirmatrelvir, an orally available covalent inhibitor of 3CL^{pro}, forms a reversible thioimidate adduct with the catalytic Cys145 (Fig. 1a) (13). Similarly, peptidomimetic and non-peptidic inhibitors of 3CL^{pro} have been developed bearing a variety of warheads: aldehydes, α-acyloxy-, α-heteroaryl- and α-hydroxy-substituted ketones (14), α-haloacetamides, α-ketoamides, α,β-unsaturated ketones, activated esters and others (10, 15, 16). Acyloxymethylketones, which have been studied as cathepsin B inhibitors (17, 18) and as activity-based probes for cysteine protease profiling (19), are also extensively explored as 3CL^{pro} inhibitors (20, 21) (Fig. 1b,c).

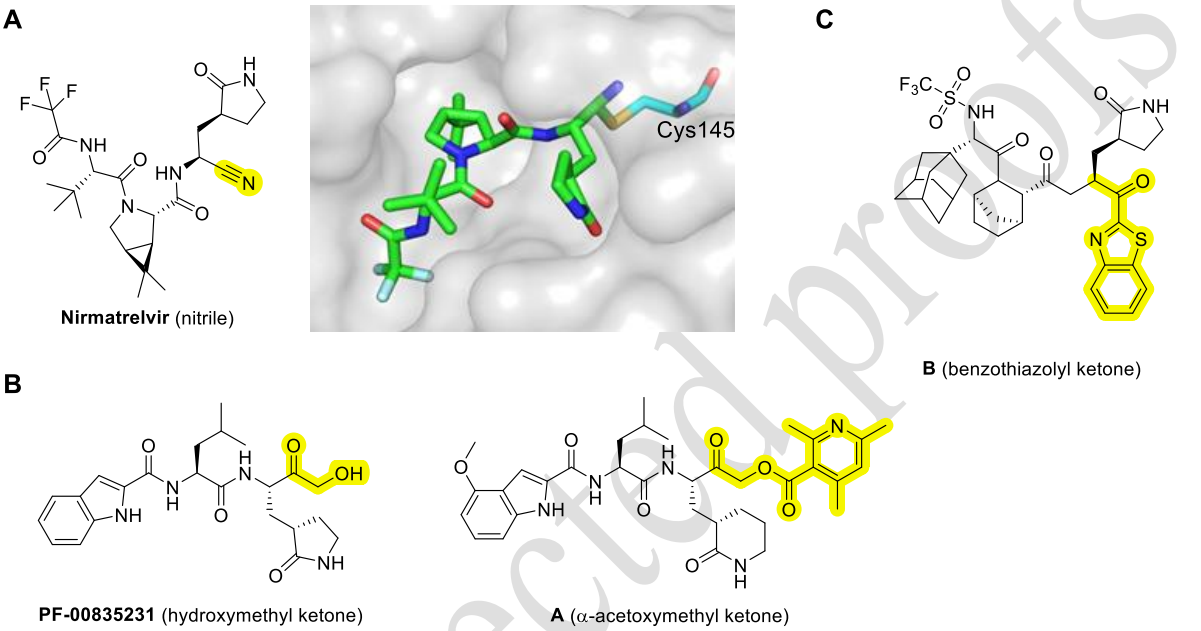

Fig. 1. 3CL^{pro} inhibitors: a) nirmatrelvir and the resolved crystal structure (PDB code 7RFS) (13); b) hydroxymethyl ketone **PF-00835231** and α-acetoxymethyl ketone **A** (20); c) benzothiazolyl ketone **B** (14). Covalent warheads are highlighted in yellow.

A rational and systematic computational approach reported by the Wolber group led to the identification of the covalently binding fragment **F1**, which inhibits the enteroviral cysteine 3C protease (Fig. 2a). Scaffold hopping subsequently yielded fragment **C5**, an α-phenylthiomethyl ketone (Fig. 2a), which covalently binds to Cys147 of the 3C protease, as confirmed by mass spectrometry (22). Recently, thiazolyl ketones have also been reported as inhibitors of cytosolic phospholipase A2α (23). A structurally related α-heteroarylthiomethylketo moiety is also present in the selective cathepsin X inhibitor **Z9** developed by Pečar Fonović *et al.* (Fig. 2b) (24). In contrast to the α-phenylthiomethyl ketones and the analogues developed by the Wolber group, **Z9** is a reversible inhibitor, as demonstrated by enzyme kinetics and reversibility assay (24). Further optimization and structure-activity relationship (SAR) studies explored the relevant chemical space; however, the inhibitory potencies against cathepsin X and the biological activities in cellular models of the analogues remained comparable to those of **Z9** (25). In addition to the inhibition of cathepsin X, α-(hetero)arythiomethyl ketones are also described in the literature as covalent and noncovalent inhibitors for various biological applications. Fragment screening by native mass spectrometry identified 3-substituted 1,2,4-triazole (**A**) as a noncovalent, zinc-binding chemotype that inhibits carbonic anhydrase II (Fig. 2c), a validated target in the management of glaucoma and congestive heart failure (26). In addition, these compounds inhibit urease (**A2**–**5**, Fig. 2c) (27), fungal H+-ATPase (28) and are disclosed as antiviral and antibacterial agents (29).

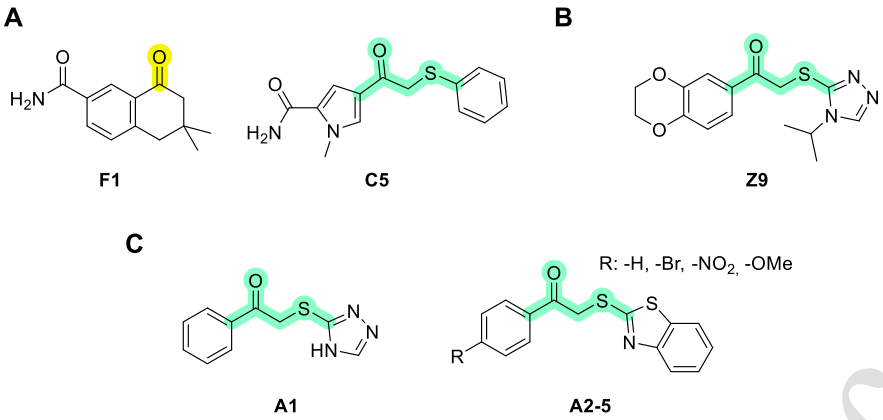

Fig. 2. (Hetero)arylthiomethyl ketones: a) ketone fragment **F1** and phenylthiomethyl ketone **C5** (22); b) cathepsin X inhibitor **Z9** (24); c) heteroarylthiomethy ketones are described as inhibitors of carbonic anhydrase II (**A1**) (26) and urease (**A2**–**5**) (27).

An *in-house* library of α-heteroarylthiomethyl ketones available at our Faculty, structurally related to previously reported α-hydroxymethyl ketone- and α-acetoxymethyl ketone-based 3CL^{pro} inhibitors, was therefore screened against the recombinant SARS-CoV-2 main protease 3CL^{pro}. The identified hit compounds inhibited 3CL^{pro} in the micromolar range and are tentatively proposed to act as covalent inhibitors.

EXPERIMENTAL

Biochemical evaluation

Cloning, expression and purification of recombinant 3CL^{pro}. – A codon optimized synthetic gene encoding the SARS–CoV-2 3CL^{pro} protease (Integrated DNA Technologies, USA) was cloned into the pET-28c(+) plasmid, and used to transform *E. coli NiCo21(DE3)* (New England Biolabs, USA). Transformed cultures were cultivated in Lysogeny broth (LB) medium supplemented with 50 μg mL^{-1} kanamycin at 37 °C and 250 rpm until reaching optical density at 600 nm (OD_{600}) of approximately 1.8. Cultures were subsequently cooled on ice (0–4 °C) for 10 min, and 3CL^{pro} protease expression was induced by the addition of 200 μmol L^{-1} isopropyl β-D-1-thiogalactopyranoside (IPTG). Expression proceeded for 24 h at 16 °C and 250 rpm. Then, cells were harvested by centrifugation (2 × 10 min, 3000 × *g*, 4 °C), and the resulting pellet resuspended in buffer A (20 mmol L^{-1} Tris-HCl, pH 7.5, 0.05 mmol L^{-1} EDTA, 2.5 mmol L^{-1} DTT, 10 % glycerol). Cell lysis was performed on ice *via* sonication, and the lysate was clarified by centrifugation (2 × 30 min, 16000 × *g*, 4 °C). The supernatant was filtered through a 100-kDa molecular weight cut-off (MWCO) centrifugal unit (Amicon Ultra-15; Merck, Germany). Ammonium sulfate was gradually added to the filtrate to a final concentration of 500 mmol L^{-1}, and the solution was loaded onto a 1 mL HiTrap Phenyl HP column (Cytiva, USA) pre-equilibrated with buffer B (50 mmol L^{-1} Tris-HCl, pH 7.5, 0.5 mol L^{-1} $(NH_4)_2SO_4$, 0.05 mmol L^{-1} EDTA, 2.5 mmol L^{-1} DTT, 10 % glycerol). After washing the column with 20 volumes of buffer B, the bound 3CL^{pro} was eluted using a linear gradient into buffer A. Eluted faction were concentrated using a 30-kDa MWCO centrifugal filter unit (Amicon Ultra-4; Merck), frozen in liquid N_2, and stored at −80 °C. Protein concentration was determined by UV-absorbance at 280 nm, using the extinction coefficient of 34380 M^{-1} cm^{-1}. Purity of 3CL^{pro} was assessed by SDS-PAGE.

Enzyme activity assay. – 3CL^{pro} protease activity was measured by kinetic assay using FRET fluorogenic substrates Dabcyl-KTSAVLQSGFRKME-Edans (Dabcyl-Lys-SARS-CoV2 Replicase pp1ab(3235-3246)-Glu-EDANS, CPC Scientific, USA) and Hilyte™Fluor488-ESATLQSGLRKAKQXL®520 (Hilyte™Fluor488, Anaspec, USA). Measurements were performed in 50 mmol L^{-1} Tris-HCl, pH 7.3, 1 mmol L^{-1} EDTA, 0.05 % Triton X-114. For the screening, compounds were pre-incubated at a concentration of 500 μmol L^{-1} with 3CL^{pro} (final concentration, 50 nmol L^{-1}) for 30 min at 30 °C. The reaction was started by adding Dabcyl-KTSAVLQSGFRKME-Edans (final concentration, 20 μmol L^{-1}), and the increase in fluorescence intensity was measured using microplate reader Synergy H4 (BioTek Instruments Inc., USA) at λ_{ex} = 360 (bandwidth, 17 nm) and λ_{em} = 528 (bandwidth, 17 nm). Final concentration of DMSO was always 10 % (*V/V*). In control experiments,

the compound was replaced by DMSO. For the blank determination (*b*), the enzyme was replaced with assay buffer. Initial velocities (*v*) were calculated from the linear trends obtained, with each measurement performed in duplicate. Inhibitory potencies were expressed as residual activities – RAs = $(v_i - b)/(v_o - b)$, where v_i represents the velocity of enzyme reaction in the presence of the test compound, and v_0 the control velocity in the presence of DMSO. To confirm the activity of the compounds and to exclude assay spectral interference at 360 nm, the active compounds from the screening phase (RA at 500 μmol L^{-1} < 50 %) were evaluated using the above described procedure by replacing Dabcyl-KTSAVLQSGFRKME-Edans substrate with Hilyte™Fluor488-ESATLQSGLRKAKQXL®520 substrate (final concentration, 2 μmol L^{-1}). For the active compound (RA at 500 μmol L^{-1} < 50 %, Hilyte™Fluor488-ESATLQSGLRKAKQXL®520 substrate), IC_{50} values using both substrates were determined by measuring RAs at seven to twelve concentrations of the compound. The IC_{50} values were calculated by fitting RAs at different concentrations to a 4-parameter logistic function [Y = Bottom + (Top – Bottom)/(1 + 10^((LogIC_{50} – X)×HillSlope), where Y represent RAs and X the $\log_{10}$ of compound concentration] using GraphPad Prism 10.4 (GraphPad Software Inc., USA). For progress curve analysis, the assays were performed by preincubating a serial dilution of compounds in the presence of the substrate Dabcyl-KTSAVLQSGFRKME-Edans (final concentration, 15 μmol L^{-1}) for 15 min at 30 °C prior to the addition of $3CL^{pro}$ (final concentration, 10 nmol L^{-1}). The increase in fluorescence intensity was followed as described above. To determine k_{obs} values, the progress curves obtained were fitted to the equation $Y = v + Vo \times [1 - \exp(-k_{obs} \times X)] / k_{obs}$. The first-order rate constants k_{obs} for GC376 (control inhibitor) were then fitted to $k_{obs} = k + (k_{inact} \times [\text{Inhibitor}])/(K_I + [\text{Inhibitor}])$. Since compounds **31** and **33** are slow and inefficient inhibitors of $3CL^{pro}$, the k_{obs} was fitted to simple linear regression, where the slope of the line equals k_{inact}/K_I (30). All fittings were performed in GraphPad Prism 10.4 (GraphPad Software Inc., USA).

Thiol reactivity assay – DTNB assay. – The assay was performed according to previously reported procedure (31). Briefly, experiments were performed in duplicate in 96-well microplates in assay buffer (20 mM sodium phosphate, 150 mM NaCl, pH 7.4). Reagent solutions were prepared freshly prior to the experiments. 2-Chloro-*N*-(3-chlorophenyl)acetamide was used as a control compound.

Thiol reactivity assay – TNB^{2-} assay. – The assay was performed according to previously reported procedure (31). Briefly, 100 μmol L^{-1} of compound was incubated in a mixture of 50 μmol L^{-1} TNB^{2-} in assay buffer containing 5 % final DMSO concentration at 37 °C. Absorbance at 412 nm was measured at 5-minute intervals for 14–21 h using microplate reader Synergy H4 (BioTek Instruments, Inc., USA) to monitor TNB^{2-} depletion. To determine the baseline drift due to the oxidation of TNB^{2-} to DTNB, blank experiment was performed, where 100 % DMSO replaced the compound. Baseline drift due to TNB^{2-} oxidation and compound background absorbances were subtracted from each measurement.

RESULTS AND DISCUSSION

The *in-house* library of fully characterized α-heteroarylthiomethyl ketones, synthetic intermediates and close analogues (compounds **1**–**38**, Table I) from the cathepsin X campaign (25) was screened for inhibition of the recombinant SARS-CoV-2 main protease $3Cl^{pro}$, which was cloned, expressed and purified as previously described (31). The initial screening was conducted at a compound concentration of 500 μmol L^{-1} with a 30-minute preincubation and using the fluorogenic substrate Dabcyl-KTSAVLQSGFRKME-EDANS (*Dabcyl-EDANS*). Compounds with residual activities (RAs) below 50 % were considered hits (Table I).

Given the relatively low excitation wavelength of the Dabcyl-EDANS substrate, *i.e.* at 360 nm, potential interference with assay readout due to the inner filter effect was considered (32). To address this, the absorbance spectra of active compounds were recorded at 500 μmol L^{-1}. Spectral interferences (*i.e.* absorbance > 0.1 AU at 360 nm) were observed for compounds **22**, **32** and **37**. All active compounds were subsequently retested under identical conditions using the HiLyte™Fluor488-QXL520 substrate, which has a higher excitation wavelength (~490 nm) and is less prone to spectral interference, even with lightly colored yellow compounds. For all active compounds, IC_{50} values were determined using both substrates.

Of the 38 compounds tested, eleven inhibited $3CL^{pro}$ with IC_{50} values below 500 μmol L^{-1} (Table I). Among the 1-(2,3-dihydrobenzo[*b*][1,4]dioxin-6-yl)ethan-1-ones **1**–**21**, only the (4*H*-1,2,4-triazol-3-yl)thio analogues bearing 4-isopropyl and 4-ethyl substitutions inhibited $3CL^{pro}$. In contrast, the analogues with smaller, unsubstituted triazoles, imidazoles, or 4-aryl-substituted 4*H*-1,2,4-triazololes were inactive. Substitution at

position 3 of the 4*H*-1,2,4-triazole, such as cyclohexyl (**18**) or phenyl (**19**), was also not tolerated, indicating a narrow structure-activity window for modifications at the heteroarylthio moiety. Notably, reduction of the ketone group in compound **1** to the corresponding racemic secondary alcohol **2** abolished inhibitory activity, underscoring the essential role of the ketone functionality for inhibition of $3CL^{pro}$. In contrast, neither the α-hydroxymethyl ketone **21** nor the thiol **22** inhibited the enzyme, suggesting that the presence of either the thiol and ketone alone is insufficient for $3CL^{pro}$ inhibition, although such functionalities have been described in the literature as effective covalent inhibitors (33). Replacement of the 2,3-dihydrobenzo[*b*][1,4]dioxine moiety by smaller fragments such as substituted phenyl groups (compounds **23**–**38**) was tolerated when the substituents were smaller (e.g. methyl, methoxy, hydroxy, nitro) and on *para* or *meta* position relative to the ketone. Among the compounds tested, *p*-tolyl and phenyl derivatives **31** and **33**, respectively, were the most potent inhibitors, with IC_{50} values of 95.4 ± 3.1 and 95.0 ± 6.9 µmol L^{-1}, respectively.

Table I. Structures of compounds and inhibition of $3CL^{pro}$ expressed as residual activities (RAs) and IC_{50} values

Compd.	Structure	$3CL^{pro}$ inhibition RA (%) at 500 µmol L^{-1}[a] IC_{50} ± SEM (µmol L^{-1})[b]	
		Substrate: Dabcyl-EDANS	Substrate: HiLyte™Fluor488-QXL520
1 **(Z9)**	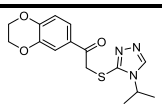	19.0 247.5 ± 15.9	30.0 153.5 ± 11.7
2	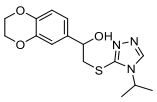	84.0	n.t.[c]
3	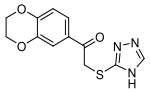	55.7	n.t.[c]
4	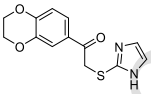	62.6	n.t.[c]
5	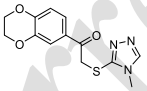	60.5	n.t.[c]
6	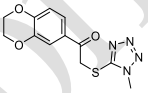	66.1	n.t.[c]
7	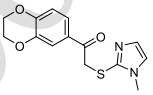	56.0	n.t.[c]
8	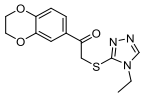	30.2 284.8 ± 52.6	36.6 255.9 ± 38.2
9	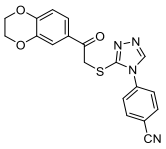	62.4	n.t.[c]
10	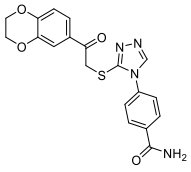	69.7	n.t.[c]

11	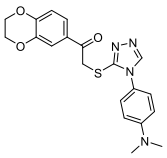	87.2	n.t.[c]
12	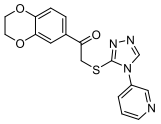	70.7	n.t.[c]
13	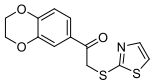	75.8	n.t.[c]
14	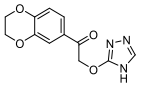	108.8	n.t.[c]
15	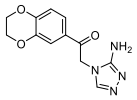	88.0	n.t.[c]
16	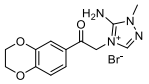	79.1	n.t.[c]
17	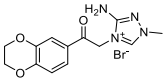	69.4	n.t.[c]
18	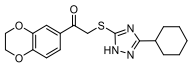	69.5	n.t.[c]
19	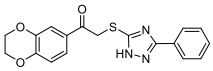	59.0	n.t.[c]
20	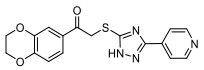	46.3 [d]	69.5
21	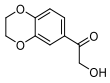	76.2	n.t.[c]
22		88.9	n.t.[c]
23	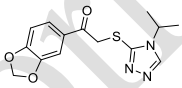	39.2 190.0 ± 11.3	35.5 186.9 ± 11.1
24	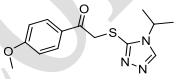	38.5 145.7 ± 14.3	30.2 131.6 ± 6.8
25	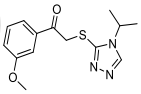	40.3 139.0 ± 10.1	32.1 155.2 ± 9.4
26	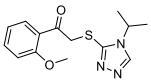	90.1	n.t.[c]
27	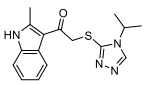	104.0	n.t.[c]
28	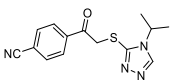	43.2 554.2 ± 68.2	58.1 426.2 ± 36.8
29	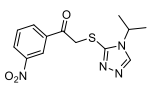	20.1 144.7 ± 7.4	45.0 181.3 ± 20.6
30	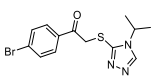	67.9	n.t.[c]
31	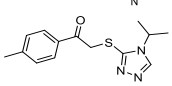	1.2 95.4 ± 3.1	24.5 129.2 ± 7.0

32	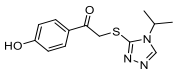	6.1 [d]	43.7 194.9 ± 19.8
33	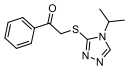	2.1 95.0 ± 6.9	33.3 153.1 ± 8.9
34	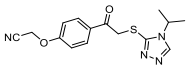	77.0	n.t.[c]
35	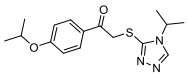	59.6	n.t.[c]
36	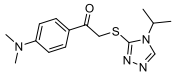	4.4 [d]	38.4 358.0 ± 26.6
37	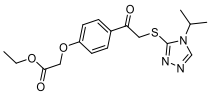	62.8	n.t.[c]
38	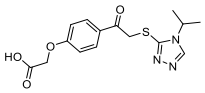	80.6	n.t.[c]

[a] RAs are means of single experiment performed in duplicate; standard deviation for RAs was < 10 %. [b] IC_{50}s are means ± standard error of the mean (SEM) for two independent experiments, each performed in duplicate. Aldehyde bisulfite GC376 and α-ketoamide boceprevir (34) were used as a positive controls (IC_{50}(*Dabcyl-EDANS substrate*) = 0.05081 ± 0.0041 and 3.977 ± 0.1444 μmol L^{-1}, respectively). [c] n.t. – not tested. [d] Assay spectral interference at 360 nm.

Based on the literature reports, the expected mechanism of action for the compounds investigated involves either covalent modification *via* the ketone moiety or a nucleophilic substitution followed by elimination of the nucleofuge, the hetero(ary)thiole (20, 22, 35). To evaluate the intrinsic reactivity of the compounds in non-proteinaceous environment *in vitro*, a thiol-containing colorimetric probe, 5-mercapto-2-nitrobenzoic acid (TNB^{2-}), was employed as a cysteine surrogate. TNB^{2-} was generated *in situ* by reduction of 5,5'-dithio-bis(2-nitrobenzoic acid) (DTNB) with tris(2-carboxyethyl)phosphine (TCEP). However, since TCEP itself is a phosphine nucleophile and could potentially react with the electrophilic compounds under investigation, an alternative assay was conducted using commercially available TNB^{2-} to avoid interference (36). Under the experimental conditions applied, none of the compounds, with the exception of fragments **21** and **22**, exhibited reactivity towards TNB^{2-}. Nonetheless, it should be noted that cysteine reactivity in a protein environment is influenced by local electronic effects in the active site of the enzyme (37). Consequently, the results obtained using thiol surrogate compounds should be interpreted with caution.

Although IC_{50} values are commonly used in medicinal chemistry to compare the inhibitory potency of compounds under standardized conditions, a detailed kinetic evaluation is more appropriate for covalent inhibitors (38). The progress curves for the hydrolysis of Dabcyl-KTSAVLQSGFRKME-Edans substrate by $3CL^{pro}$ indicated that covalent inactivation by inhibitors **31** and **33** is rather slow and inefficient, particularly when compared to the reference inhibitor CG376 (Fig. 3) (39). Nevertheless, further optimization and comprehensive characterization are required before the proposed mechanism of action can be conclusively confirmed. Covalent mode should be confirmed by mass spectrometry to verify modification of the catalytic Cys145. Secondly, establishing the pre-reaction binding pose of the intact inhibitor through molecular modeling would further aid in understanding key interactions in the $3CL^{pro}$'s active site. These insights could then guide the rational optimization of α-heteroarylthiomethyl ketones to enhance their potency and selectivity toward the targets. Key findings regarding structure-activity relationship and plausible further steps to improve inhibitory activities based on the data presented herein are presented in Fig. 4.

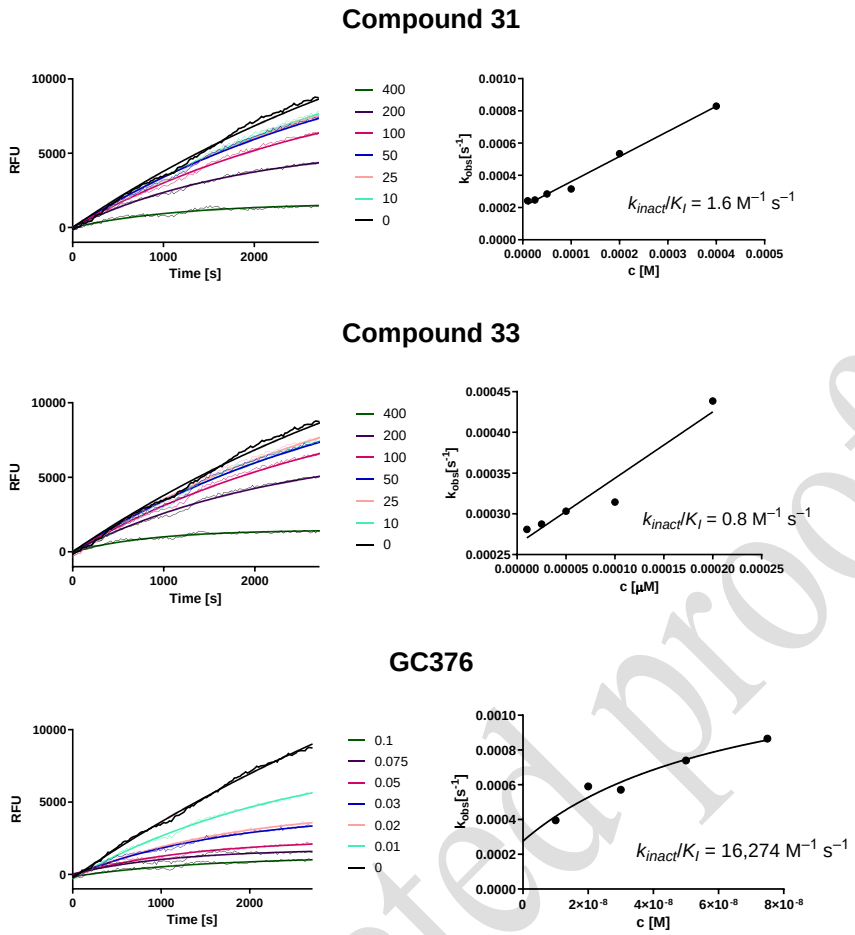

Fig. 3. Progress curve analysis. Left: progress curves of 3CL^{pro} reaction in the absence or presence of indicated concentrations (in μmol L^{-1}) of inhibitors; Right: Secondary plot of k_{obs} as a function of inhibitor concentration.

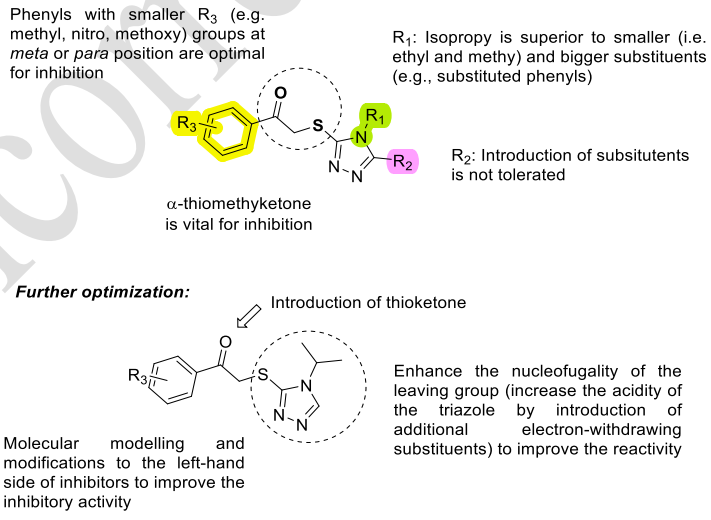

Fig. 4. Key structural-activity relationship findings for 3CL^{pro} inhibition and proposed directions for further optimization.

CONCLUSIONS

Small, academic *in-house* compound libraries, often compiled from previous medicinal chemistry projects, represent a valuable resource for the identification of novel hits against disease-relevant targets. Here, we present an example of cathepsin X focused compound library, which was screened to identify structurally novel inhibitors of the SARS-CoV2 main protease $3CL^{pro}$. Preliminary *in vitro* evaluation, together with supporting literature data, suggest a covalent mode of action. This hypothesis warrants further experimental confirmation by native and before proceeding with SARs optimization and broader biological evaluation.

Acknowledgements and funding. – This work was funded by the Slovenian Research and Innovation Agency (research core funding No. P1-0208).

Conflict of interest. – The authors declare no conflict of interest.

Authors contributions. – Conceptualization, D.K. and S.G.; biochemical experiments, D.K., M.P., and K.B.; writing, original draft preparation, D.K.; writing, review and editing, D.K., M.P, K.B., and S.G.; supervision, S.G. and D.K; funding, S.G. All authors have read and agreed to the published version of the manuscript.

REFERENCES

1. C. I. Paules, H. D. Marston and A. S. Fauci, Coronavirus infections-more than just the common cold, *JAMA* **323**(8) (2020) 707–708; https://doi.org/10.1001/jama.2020.0757
2. V. C. C. Cheng, S. K. P. Lau, P. C. Y. Woo and K. Y. Yuen, Severe acute respiratory syndrome coronavirus as an agent of emerging and reemerging infection, *Clin. MicroBiol. Rev.* **20**(4) (2007) 660–694; https://doi.org/10.1128/CMR.00023-07
3. Y.-Z. Zhang and E. C. Holmes, A genomic perspective on the origin and emergence of SARS-CoV-2, Cell **181**(2) (2020) 223–227; https://doi.org/10.1016/j.cell.2020.03.035
4. A. Faramarzi, S. Norouzi, H. Dehdarirad, S. Aghlmand, H. Yusefzadeh and J. Javan-Noughabi, The global economic burden of COVID-19 disease: a comprehensive systematic Review and meta-analysis, *Syst. Rev.* **13**(1) (2024) Article ID 68 (10 pages); https://doi.org/10.1186/s13643-024-02476-6
5. A. Pišlar, A. Mitrović, J. Sabotič, U. Pečar Fonović, M. Perišić Nanut, T. Jakoš, E. Senjor and J. Kos, The role of cysteine peptidases in coronavirus cell entry and replication: The therapeutic potential of cathepsin inhibitors, *PLoS Pathog.* **16**(11) (2020) e1009013 (23 pages); https://doi.org/10.1371/journal.ppat.1009013
6. H. Hoenigsperger, R. Sivarajan and K. M. Sparrer, Differences and similarities between innate immune evasion strategies of human coronaviruses, *Curr. Opin. Microbiol.* **79** (2024) Article ID 102466 (11 pages); https://doi.org/10.1016/j.mib.2024.102466
7. J. C. Ferreira, S. Fadl and W. M. Rabeh, Key dimer interface residues impact the catalytic activity of 3CLpro, the main protease of SARS-CoV-2, *J. Biol. Chem.* **298**(6) (2022) 102023; https://doi.org/10.1016/j.jbc.2022.102023
8. N. Atatreh, R. E. Mahgoub and M. A. Ghattas, Exploring covalent inhibitors of SARS-CoV-2 main protease: from peptidomimetics to novel scaffolds, *J. Enzyme Inhib. Med. Chem.* **40**(1) (2025) Article ID 2460045 (26 pages); https://doi.org/10.1080/14756366.2025.2460045
9. Y. Yang, Y.-D. Luo, C.-B. Zhang, Y. Xiang, X.-Y. Bai, D. Zhang, Z.-Y. Fu, R.-B. Hao and X.-L. Liu, Progress in research on inhibitors targeting SARS-CoV-2 main protease (Mpro), *ACS Omega* **9**(32) (2024) 34196–34219; https://doi.org/10.1021/acsomega.4c03023
10. Y.-Q. Xiao, J. Long, S.-S. Zhang, Y.-Y. Zhu and S.-X. Gu, Non-peptidic inhibitors targeting SARS-CoV-2 main protease: a Review, Bioorg. Chem. **147** (2024) 107380; https://doi.org/10.1016/j.bioorg.2024.107380
11. O. Ebenezer and M. Shapi, Promising inhibitors against main protease of SARS CoV-2 from medicinal plants: in silico identification, *Acta Pharm.* **72**(2) (2022) 159–169; https://doi.org/10.2478/acph-2022-0020
12. M. H. Choi, E. Y. F. Wan, I. C. K. Wong, E. W. Y. Chan, W. M. Chu, A. R. Tam, K. Y. Yuen and I. F. N. Hung, Comparative effectiveness of combination therapy with nirmatrelvir-ritonavir and remdesivir versus monotherapy with remdesivir or nirmatrelvir-ritonavir in patients hospitalised with COVID-19: A target trial emulation study, *Lancet Infect. Dis.* **24**(11) (2024) 1213–1224; https://doi.org/10.1016/S1473-3099(24)00353-0
13. D. R. Owen, C. M. N. Allerton, A. S. Anderson, L. Aschenbrenner, M. Avery, S. Berritt, B. Boras, R. D. Cardin, A. Carlo, K. J. Coffman, A. Dantonio, L. Di, H. Eng, R. Ferre, K. S. Gajiwala, S. A. Gibson, S. E. Greasley, B. L. Hurst, E. P. Kadar, A. S. Kalgutkar, J. C. Lee, J. Lee, W. Liu, S. W. Mason, S. Noell, J. J. Novak, R. S. Obach, K. Ogilvie, N. C. Patel, M. Pettersson, D. K. Rai, M. R. Reese, M. F. Sammons, J. G. Sathish, R. S. P. Singh, C. M. Steppan, A. E. Stewart, J. B. Tuttle, L. Updyke, P. R. Verhoest, L. Wei, Q. Yang

and Y. Zhu, An oral SARS-CoV-2 Mpro inhibitor clinical candidate for the treatment of COVID-19, *Science* **374**(6575) (2021) 1586–1593; https://doi.org/10.1126/science.abl4784
14. H. Yang, M. You, X. Shu, J. Zhen, M. Zhu, T. Fu, Y. Zhang, X. Jiang, L. Zhang, Y. Xu, Y. Zhang, H. Su, Q. Zhang and J. Shen, Design, synthesis and biological evaluation of peptidomimetic benzothiazolyl ketones as 3CLpro inhibitors against SARS-CoV-2, *Eur. J. Med. Chem.* **257** (2023) Article ID 115512 (13 pages); https://doi.org/10.1016/j.ejmech.2023.115512
15. A. M. Shawky, F. A. Almalki, H. A. Alzahrani, A. N. Abdalla, B. G. M. Youssif, N. A. Ibrahim, M. Gamal, H. A. M. El-Sherief, M. M. Abdel-Fattah, A. A. Hefny, A. H. Abdelazeem and A. M. Gouda, Covalent small-molecule inhibitors of SARS-CoV-2 Mpro: Insights into their design, classification, biological activity, and binding interactions, *Eur. J. Med. Chem.* **277** (2024) Article ID 116704; https://doi.org/10.1016/j.ejmech.2024.116704
16. X. Li and Y. Song, Structure and function of SARS-CoV and SARS-CoV-2 main proteases and their inhibition: A comprehensive review, *Eur. J. Med. Chem.* **260** (2023) Article ID 115772 (53 pages); https://doi.org/10.1016/j.ejmech.2023.115772
17. A. Krantz, L. J. Copp, P. J. Coles, R. A. Smith and S. B. Heard, Peptidyl (acyloxy)methyl ketones and the quiescent affinity label concept: The departing group as a variable structural element in the design of inactivators of cysteine proteinases, *Biochemistry* **30**(19) (1991) 4678–4687; https://doi.org/10.1021/bi00233a007
18. B. M. Wagner, R. A. Smith, P. J. Coles, L. J. Copp, M. J. Ernest and A. Krantz, In vivo inhibition of cathepsin B by peptidyl (acyloxy)methyl ketones, *J. Med. Chem.* **37**(12) (1994) 1833–1840; https://doi.org/10.1021/jm00038a012
19. A. G. Coman, C. C. Paraschivescu, N. D. Hadade, A. Juncu, O. Vlaicu, C.-I. Popescu and M. Matache, New acyloxymethyl ketones: useful probes for cysteine protease profiling, *Synthesis* **48**(22) (2016) 3917–3923; https://doi.org/10.1055/s-0035-1562781
20. R. L. Hoffman, R. S. Kania, M. A. Brothers, J. F. Davies, R. A. Ferre, K. S. Gajiwala, M. He, R. J. Hogan, K. Kozminski, L. Y. Li, J. W. Lockner, J. Lou, M. T. Marra, L. J. Mitchell, B. W. Murray, J. A. Nieman, S. Noell, S. P. Planken, T. Rowe, K. Ryan, G. J. Smith III, G. J. Solowiej, C. M. Steppan and B. Taggart, Discovery of ketone-based covalent inhibitors of coronavirus 3CL proteases for the potential therapeutic treatment of COVID-19, *J. Med. Chem.* **63**(21) (2020) 12725–12747; https://doi.org/10.1021/acs.jmedchem.0c01063
21. M. A. T. van de Plassche, M. Barniol-Xicota and S. H. L. Verhelst, Peptidyl acyloxymethyl ketones as activity-based probes for the main protease of SARS-CoV-2, *ChembioChem.* **21**(23) (2020) 3383–3388; https://doi.org/10.1002/cbic.202000371
22. R. Schulz, A. Atef, D. Becker, F. Gottschalk, C. Tauber, S. Wagner, C. Arkona, A. A. Abdel-Hafez, H. H. Farag, J. Rademann and G. Wolber, Phenylthiomethyl ketone-based fragments show selective and irreversible inhibition of enteroviral 3C proteases, *J. Med. Chem.* **61**(3) (2018) 1218–1230; https://doi.org/10.1021/acs.jmedchem.7b01440
23. F. J. Ashcroft, A. Bourboula, N. Mahammad, E. Barbayianni, A. J. Feuerherm, T. T. Nguyen, D. Hayashi, M. G. Kokotou, K. Alevizopoulos, E. A. Dennis, G. Kokotos and B. Johansen, Next generation thiazolyl ketone inhibitors of cytosolic phospholipase A2 α for targeted cancer therapy, *Nat. Commun.* **16**(1) (2025) Article ID 164 (16 pages); https://doi.org/10.1038/s41467-024-55536-9
24. U. P. Fonović, A. Mitrović, D. Knez, T. Jakoš, A. Pišlar, B. Brus, B. Doljak, J. Stojan, S. Žakelj, J. Trontelj, S. Gobec and J. Kos, Identification and characterization of the novel reversible and selective cathepsin X inhibitors, *Sci. Rep.* **7**(1) (2017) Article ID 11459 (11 pages); https://doi.org/10.1038/s41598-017-11935-1
25. U. P. Fonović, D. Knez, M. Hrast, N. Zidar, M. Proj, S. Gobec and J. Kos, Structure-activity relationships of triazole-benzodioxine inhibitors of cathepsin X, *Eur. J. Med. Chem.* **193** (2020) Article ID 112218 (17 pages); https://doi.org/10.1016/j.ejmech.2020.112218
26. L. A. Woods, O. Dolezal, B. Ren, J. H. Ryan, T. S. Peat and S.-A. Poulsen, Native state mass spectrometry, surface plasmon resonance, and X-ray crystallography correlate strongly as a fragment screening combination, *J. Med. Chem.* **59**(5) (2016) 2192–2204; https://doi.org/10.1021/acs.jmedchem.5b01940
27. M. Özil, Ö. Tuzcuoğlu, M. Emirik and N. Baltaş, Developing a scaffold for urease inhibition based on benzothiazoles: Synthesis, docking analysis, and therapeutic potential, *Arch. Pharm.* (Weinheim) **354**(12) (2021) e2100200; https://doi.org/10.1002/ardp.202100200
28. T.-T. Tung, T. T. Dao, M. G. Junyent, M. Palmgren, T. Günther-Pomorski, A. T. Fuglsang, S. B. Christensen and J. Nielsen, LEGO-inspired drug design: Unveiling a class of benzo[d]thiazoles containing a 3,4-dihydroxyphenyl moiety as plasma membrane H+-ATPase inhibitors, *ChemMedChem.* **13**(1) (2018) 37–47; https://doi.org/10.1002/cmdc.201700635
29. T. T. Thanh, H. L. Xuan and T. N. Quoc, Benzo[d]thiazole-2-thiol bearing 2-oxo-2-substituted-phenylethan-1-yl as potent selective lasB quorum sensing inhibitors of Gram-negative bacteria, *RSC Adv.* **11**(46) (2021) 28797–28808; https://doi.org/10.1039/d1ra03616e

30. C. M. Harris, S. E. Foley, E. R. Goedken, M. Michalak, S. Murdock and N. S. Wilson, Merits and pitfalls in the characterization of covalent inhibitors of Bruton's tyrosine kinase, *SLAS Discov.* **23**(10) (2018) 1040–1050; https://doi.org/10.1177/2472555218787445
31. M. Proj, M. Hrast, D. Knez, K. Bozovičar, K. Grabrijan, A. Meden, S. Gobec and R. Frlan, Fragment-sized thiazoles in fragment-based drug discovery campaigns: friend or Foe?, *ACS Med. Chem. Lett*. **13**(12) (2022) 1905–1910; https://doi.org/10.1021/acsmedchemlett.2c00429
32. A. Simeonov and M. I. Davis, *Interference with Fluorescence and Absorbance,* in *Assay Guidance Manual* (Eds. S. Markossian, A. Grossman, K. Brimacombe, M. Arkin, D. Auld, C. Austin, J. Baell), Eli Lilly & Company and the National Center for Advancing Translational Sciences, Bethesda 2004.
33. R. W. Marquis, Y. Ru, J. Zeng, R. E. Trout, S. M. LoCastro, A. D. Gribble, J. Witherington, A. E. Fenwick, B. Garnier, T. Tomaszek, D. Tew, M. E. Hemling, C. J. Quinn, W. W. Smith, B. Zhao, M. S. McQueney, C. A. Janson, K. D'Alessio and D. F. Veber, Cyclic ketone inhibitors of the cysteine protease cathepsin K, *J. Med. Chem.* **44**(5) (2001) 725–736; https://doi.org/10.1021/jm000320t
34. L. Fu, F. Ye, Y. Feng, F. Yu, Q. Wang, Y. Wu, C. Zhao, H. Sun, B. Huang, P. Niu, H. Song, Y. Shi, X. Li, W. Tan, J. Qi and G. F. Gao, Both BocepRev.ir and GC376 efficaciously inhibit SARS-CoV-2 by targeting its main protease, *Nat. Commun.* **11**(1) (2020) Article ID 4417 (8 pages); https://doi.org/10.1038/s41467-020-18233-x
35. R. Justin Grams, K. Yuan, M. W. Founds, M. L. Ware, M. G. Pilar and K.-L. Hsu, Imidazoles are tunable nucleofuges for developing tyrosine-reactive electrophiles, *ChemBioChem.* **25**(16) (2024) e202400382; https://doi.org/10.1002/cbic.202400382
36. M. Proj, D. Knez, I. Sosič and S. Gobec, Redox active or thiol reactive? Optimization of rapid screens to identify less evident nuisance compounds, *Drug Discov. Today* **27**(6) (2022) 1733–1742; https://doi.org/10.1016/j.drudis.2022.03.008
37. V. Vaissier Welborn, Understanding cysteine reactivity in protein environments with electric fields, *J. Phys. Chem.* B **127**(46) (2023) 9936–9942; https://doi.org/10.1021/acs.jpcb.3c05749
38. E. Mons, S. Roet, R. Q. Kim and M. P. C. Mulder, A comprehensive guide for assessing covalent inhibition in enzymatic assays illustrated with kinetic simulations, *Curr. Protoc.* **2**(6) (2022) e419 (86 pages); https://doi.org/10.1002/cpz1.419
39. H. Liu, S. Iketani, A. Zask, N. Khanizeman, E. Bednarova, F. Forouhar, B. Fowler, S. J. Hong, H. Mohri, M. S. Nair, Y. Huang, N. E. S. Tay, S. Lee, C. Karan, S. J. Resnick, C. Quinn, W. Li, H. Shion, X. Xia, J. D. Daniels, M. Bartolo-Cruz, M. Farina, P. Rajbhandari, C. Jurtschenko, M. A. Lauber, T. McDonald, M. E. Stokes, B. L. Hurst, T. Rovis, A. Chavez, D. D. Ho and B. R. Stockwell, Development of optimized drug-like small molecule inhibitors of the SARS-CoV-2 3CL protease for treatment of COVID-19, *Nat. Commun.* **13**(1) (2022) Article ID 1891 (16 pages); https://doi.org/10.1038/s41467-022-29413-2